From Quantum Chemistry and the Classical Theory of Polar Liquids to Continuum Approximations in Molecular Mechanics Calculations

SERGIO A. HASSAN,[1] ERNEST L. MEHLER[2]

[1]*Center for Molecular Modeling, Division of Computational Bioscience (CMM/DCB/CIT), National Institutes of Health, DHHS, Bethesda, Maryland 20892, USA*

[2]*Department of Physiology and Biophysics, Weill Medical College, Cornell University, New York, New York 10021, USA*

Received 18 October 2004; accepted 29 December 2004
Published online 1 February 2005 in Wiley InterScience (www.interscience.wiley.com).
DOI 10.1002/qua.20526

ABSTRACT: Biological macromolecules and other polymers belong to the class of mesoscopic systems, with characteristic length scale of the order of a nanometer. Although microscopic models would be the preferred choice in theoretical calculations, their use in computer simulations becomes prohibitive for large systems or long simulation times. On the other hand, the use of purely macroscopic models in the mesoscopic domain may introduce artifacts, with effects that are difficult to assess and that may compromise the reliability of the calculations. Here is proposed an approach with the aim of minimizing the empirical nature of continuum approximations of solvent effects within the scope of molecular mechanics (MM) approximations in mesoscopic systems. Using quantum chemical methods, the potential generated by the molecular electron density is first decomposed in a multicenter-multipole expansion around predetermined centers. The monopole and dipole terms of the expansion at each site create electric fields that polarize the surrounding aqueous medium whose dielectric properties can be described by the classical theory of polar liquids. Debye's theory allows a derivation of the dielectric profiles created around isolated point charges and dipoles that can incorporate Onsager reaction field corrections. A

Correspondence to: E. L. Mehler; e-mail: elm2020@med.cornell.edu, or S. A. Hassan; e-mail: mago@helix.nih.gov

This paper is dedicated to Dr. John Pople, whose work made such a signal contribution to transforming quantum chemistry from an esoteric specialty to a standard component of the chemist's toolbox.

Contract grant sponsor: NIH.
Contract grant number: R01 DA15170.

© 2005 Wiley Periodicals, Inc.

superposition of screened Coulomb potentials obtained from this theory makes possible a simple derivation of a formal expression for the total electrostatic energy and the polar component of the solvation energy of the system. A discussion is presented on the physical meaning of the model parameters, their transferability, and their convergence to calculable quantities in the limit of simple systems. The performance of this continuum approximation in computer calculations of amino acids in the context of an atomistic force field is discussed. Applications of a continuum model based on screened Coulomb potentials in multinanosecond simulations of peptides and proteins are briefly reviewed. © 2005 Wiley Periodicals, Inc. Int J Quantum Chem 102: 986–1001, 2005

Key words: continuum solvent; molecular mechanics; QM/MM; quantum chemistry

Introduction

Molecular interactions in biological systems occur mostly in solutions. From structure, dynamics, and thermodynamics of macromolecules to chemical equilibrium, reaction mechanisms, electronic spectra, and molecular vibrations of small molecules, the solvent plays a fundamental role. Depending on the size scale of the system, the properties to be studied and the time scale involved, different theoretical approaches are available. Nowadays, *ab initio* molecular dynamic (MD) simulation of small systems can be carried out in the picosecond time scale using a high level of theory, for example, Hartree–Fock (HF) or density functional theory (DFT) [1–4]. An example of this kind of study relevant to biological systems is the simulation recently reported of proton translocation in Bacteriorhodopsin, a transmembrane receptor that uses light to trigger a specific signal transduction pathway in the cell [5]. Upon isomerization of retinal due to photon absorption, a proton is transferred to the cell interior through a translocation mechanism that involves a short water chain in the protein interior [6]. Dynamic events spanning relatively longer time scales and/or larger molecular systems, including the solid state, can also be studied at a quantum mechanical (QM) level using, for example, the Car–Parrinello method [7, 8]. An example of this, relevant to biological chemistry, is the study of the dynamics of proton diffusion in bulk water [9]. This particular study provided insight into acid–base equilibrium, an ubiquitous phenomenon in solution chemistry and biochemistry.

As the size of the system increases and the dynamic events span time scales in the microsecond to millisecond range, it becomes necessary to introduce further approximations to the full quantum mechanical approach. Thus, molecular mechanics (MM) approximations that evolved from simple physical potentials for use in simulations of liquids to the sophisticated empirical force fields currently in use for simulations of macromolecules such as proteins and nucleic acid chains [10] have been developed. The MM methods are by and large based on classical mechanics and use empirical force fields that rely heavily on their parameterization.

The availability of MM force fields expanded considerably the range of applicability of theoretical methods to study physical effects, mainly those related to thermodynamics and statistical mechanical concepts. At the same time, however, this approximation drastically restricted or completely abolished the possibility of studying pure chemical problems, that is, phenomena that involve the breaking and formation of covalent bonds, such as enzyme catalysis and proton transfer. To partially mitigate this limitation, hybrid methods were developed that divide the system into a pure MM (classical) region and a QM region using a properly modified Hamiltonian that accommodates the MM potential (both bonded and nonbonded interactions) and its effect on the electron density in the QM region [11, 12]. This hybrid approach was first introduced in a pioneering paper by Warshel and Levitt [13]. The three levels of theory, here referred to as QM, QM/MM (the hybrid approach), and MM, have been successfully applied to the study of biological molecules. At the same time, MM force fields are continually evolving to describe the physics of the systems with an increasing degree of accuracy and realism. The main drawback with this approximation is the need to define and derive parameters for the empirical force fields. Moreover, as their quality improves it is hoped that the results become more accurate and reliable, assuming of course that the empirical energy function contains terms that represent the physics of the process to be studied. The optimization of parameters is a diffi-

cult and time-consuming task, but efforts are being made to derive high-quality parameters for bonded as well as nonbonded interaction terms in the force fields. In particular, bonded parameters for small organic molecules have been derived to reproduce experimental or *ab initio* properties in the gas phase [14–17].

Because of the enormous interest in biological processes, water, nucleic acids, and amino acids have been among the most intensively optimized systems. Parameters for nonbonded interactions such as those involved in Coulomb and Lennard–Jones potential terms have also been obtained and optimized for calculations of biological macromolecules in explicit solvent (water). However, the calculations of macromolecules immersed in explicit water rapidly exhaust computational capabilities, and it has become apparent that a way has to be found to reduce the dimensionality of the problem. One approach to do this is to replace the explicit solvent by a continuum description that is incorporated into the force field, although such models modify the form of the simple nonbonded terms valid when explicit solvent is used. At the same time, continuum models of solvent effects incorporate a new set of parameters into the force field that also require careful optimization.

The theoretical description of solvent effects in small molecules is generally based on one or another form of self-consistent reaction field theory [18–20]. Although still approximate, their limitations and scope of applicability can be reasonably well identified. However, such approaches are still computationally demanding for the larger size scale commonly found in biological systems, so that further simplifications had to be sought to make the systems amenable to computational study. As a natural consequence, this has brought into MM force fields a miscellany of methods and approximations that, due to a mismatch of parameters to the phenomena being studied, may require parameter adjustments and reparameterizations. This proliferation of models is understandable because of the growing pressure for applying "molecular modeling" techniques to macromolecular systems, which are among the most complex in nature, to solve problems that, invariably, are much too difficult. Thus, the need to understand the limitations of a particular approach and its scope of applicability (defined by the physics of the problem to be studied) has largely been neglected.

This paper addresses the question of how to bridge the gap between small and large molecules, in the development of a continuum model of solvation, by combining the classical theory of liquids with quantum chemical calculations of the solute molecule for use in MM force fields. The possibility of merging these formalisms of classical and quantum mechanics into a unique picture has the advantage that the resulting model could be applied transparently to a QM or a MM calculation where the solvent plays a role, i.e., most phenomena in chemistry and biology. At the same time, this approach would help to minimize empiricism and the lack of transferability of parameters, a drawback of MM force fields for biological systems.

This paper is organized as follows: the second section presents an overview of the two basic components of the proposed methodology for achieving the merger outlined in the previous paragraph. The first component discusses methods for assigning atomic properties in molecules: (i) Bader's theory of atoms in molecules (AIM) [21–25], and (ii) Stone's distributed multipole analysis (DMA) [26, 27]; the second component deals with the classic theory of polar/polarizable liquids [28–32] originally developed by Lorentz, Debye, Sack (LDS), and Onsager (LDSO), which is briefly reviewed. A connection with atomic properties of the solute and with the multipole expansion of the potential is discussed. In the third section the screened Coulomb potential (SCP) continuum solvent model [33] is described and the SCP-based implicit solvent model (SCP-ISM) for MM calculations of macromolecules [33–36] is reviewed. In the fourth section dielectric profiles and the associated screening functions are calculated numerically from the LDSO theory for different atomic charges. A discussion concerning the physical meaning of parameters and their definition is presented. A summary and a discussion of future direction are also given.

Atom-Based Partitioning of the Electron Density and the Classical Theory of Polar Liquids

MULTICENTER-MULTIPOLE EXPANSION OF THE POTENTIAL

The basic tool for merging a partitioning of the molecular density with the theory of polar fluids is the multicenter-multipole expansion of the potential [37]. Let $\rho(\mathbf{r})$ be a charge density distribution and expand it as a sum over a set of N arbitrary functions $\{\rho_i(\mathbf{r})\}_{i=1}^{N}$, that is,

$$\rho(\mathbf{r}) = \sum_{i=1}^{N} \rho_i(\mathbf{r}). \quad (1)$$

The electric potential $\phi(\mathbf{R})$ at any arbitrary point $\mathbf{R}$ in space is given by

$$\phi(\mathbf{R}) = \int_{\Re^3} \frac{\rho(\mathbf{r})}{|\mathbf{R}-\mathbf{r}|}\, d^3r = \sum_{i=1}^{N} \int_{\Re^3} \frac{\rho_i(\mathbf{r})}{|\mathbf{R}-\mathbf{r}|}\, d^3r = \sum_{i=1}^{N} \phi_i(\mathbf{R}). \quad (2)$$

The functions $\phi_i(\mathbf{R})$ can be thought of as the potential in $\mathbf{R}$ generated by a charge distribution $\rho_i(\mathbf{r})$. The electric field generated by $\phi(\mathbf{R})$ is given by $-\nabla\phi(\mathbf{R})$, and similarly each $\phi_i(\mathbf{R})$ can be considered to generate a field $\mathbf{E}_i(\mathbf{R})$ given by $-\nabla\phi_i(\mathbf{R})$, such that $\mathbf{E}(\mathbf{R}) = \Sigma\, \mathbf{E}_i(\mathbf{R})$. Standard methods [38] can be used to develop a multipole expansion for each $\phi_i(\mathbf{R})$ around an arbitrary point $\mathbf{R}_i$ provided that $|\mathbf{r}-\mathbf{R}_i|/|\mathbf{R}-\mathbf{R}_i| \ll 1$. For the present purpose it is necessary to retain only the first two terms of the expansion, that is, the monopole and dipolar terms:

$$\phi_i(\mathbf{R}) \approx \frac{Q_i}{\Delta R_i} + \frac{\Delta\mathbf{R}_i \cdot \boldsymbol{\mu}_i}{\Delta R_i^3}, \quad (3)$$

where $\Delta\mathbf{R}_i = \mathbf{R} - \mathbf{R}_i$, $\mathbf{r}_i = \mathbf{r} - \mathbf{R}_i$, $Q_i = \int_{\Omega_i} \rho_i(\mathbf{r}) d^3r$ and $\boldsymbol{\mu}_i = \int_{\Omega_i} \rho_i(\mathbf{r}_i + \mathbf{R}_i)\mathbf{r}_i d^3r_i$; $\Omega_i \subseteq \Re^3$.

From the definition of $\boldsymbol{\mu}_i$ it follows that

$$\boldsymbol{\mu}_i = \int_{\Omega_i} \rho_i(\mathbf{r}_i + \mathbf{R}_i)\mathbf{r}_i d^3r_i = \int_{\Gamma_i} \rho_i(\mathbf{r})\mathbf{r} d^3r - Q_i\mathbf{R}_i = \mathbf{p}_i - Q_i\mathbf{R}_i, \quad (4)$$

where $\mathbf{p}_i$ is the dipole moment of the distribution $\rho_i(\mathbf{r})$ with respect to the center $\mathbf{r} = 0$ (Γ_i is the integration domain in $\mathbf{r}$). Although $\boldsymbol{\mu}_i$ is independent of spatial transformations regardless of the values of Q_i, both $\mathbf{p}_i$ and $\mathcal{P}_i = Q_i\mathbf{R}_i$ do depend, in general, on the reference frame.

PARTITIONING OF THE MOLECULAR ELECTRON DENSITY

The continuous spatial arrangement of charge in a molecular system has a clear physical meaning because it is an observable of the system. Unfortunately, there is no unique way to partition this molecular electron charge distribution into local properties because the molecular Hamiltonian cannot be partitioned in this way. However, the idea of local properties has always been attractive because it allows for simple chemical interpretation, and a number of more or less arbitrary approaches for defining such partitioning have been proposed [21, 39–43]. Atomistic force fields used in MM simulations usually (but not always) use partial charges located on the nuclei to represent the molecular charge distribution. Thus, the goal of developing a seamless way to pass from $\rho(\mathbf{r})$ to $\rho_i(\mathbf{r})$ and finally to the point charge q_i and dipole $\mathbf{u}_i$ would be enhanced by any scheme that is based on a reasonably quantitative definition for calculating q_i and $\mathbf{u}_i$ from $\rho_i(\mathbf{r})$.

One such approach is Bader's theory of AIM [21–25]. In this approach topological properties of the electron density are used to define a set of spatial domains associated with individual atoms. Zero-flux surfaces, $\mathbf{S}(\mathbf{r})$, are defined in the system such that $\nabla\rho(\mathbf{r}) \cdot \hat{\mathbf{n}}(\mathbf{r}) = 0$, where $\hat{\mathbf{n}}(\mathbf{r})$ is a unit vector normal to $\mathbf{S}(\mathbf{r})$ at each point $\mathbf{r}$ in the space. With this definition each surface surrounds a region $\Omega_s(\mathbf{r})$ of space containing a point where $\rho(\mathbf{r})$ reaches a maximum (the atomic nucleus). Therefore, an atom, i, in the molecule is defined as the nucleus (with total charge eZ_i) plus the charge density in the associated basin $\Omega_{S_i}(\mathbf{r}) \equiv \Omega_i$ that contains it. The net atomic charge is then defined as $q_i = eZ_i + Q_i$, where the electronic charge associated with this atom is given by $Q_i = \int_{\Omega_i} \rho(\mathbf{r}) d^3r$. Although this partitioning is also arbitrary from a physical standpoint, it has unique properties that are independent of the basis set used in the QM calculations, in contrast to other approaches such as those based on population analysis. The AIM theory provides a natural way of partitioning $\rho(\mathbf{r})$ in a set of conjoint spatial regions $\{\Omega_{S_i}(\mathbf{r})\}_{i=1}^{N}$ that are univocally associated with a set of spatial densities $\{\rho_i(\mathbf{r})\}_{i=1}^{N}$ and can be used to expand $\rho(\mathbf{r})$ as in Eq. (1). Therefore, it is convenient to define the set $\{\mathbf{R}_i\}_{i=1}^{N}$ as the position of the nuclei in a molecular system composed of N atoms. With these definitions, a multicenter-multipole expansion can be performed as described above based on atomic charges and dipoles [cf. Eqs. (2)–(4)].

Other methods to quantify atomic properties in a molecule have been reported [39–42]. The problem of assigning atomic charges is closely related to the physical interpretation of a chemical bond. Real systems are somewhere in between the limits of an ideal ionic bond and an ideal covalent bond. The original

definition of atomic charges was given by the Mulliken population analysis [39]. An objection to this approach is that the dipole moment calculated with these partial charges does not converge to its expectation value, and Mulliken net charges cannot be used to define the charge distribution for MM simulations; thus, improvements have been sought to alleviate this and other drawbacks [26, 44, 45].

One approach to improve on the Mulliken population analysis is Stone's DMA [26, 27], which is a generalization of Mulliken's approximation. In this method the electrostatic potential at any point in space is represented by a set of multipole expansions centered at a number of points throughout the system, the so-called DMA sites. In general, a multicenter-multipole expansion of the potential has the advantage over a one-center expansion in that fast convergence is attained at all accessible distances from the charge distribution. Stone's DMA method relies on the Gaussian nature of the basis functions and makes use of their properties to define appropriate local quantities in the system, such as charges, dipoles, quadrupoles, etc. [27, 46]. Two main sources of arbitrariness can be recognized in this method: the choice of the expansion centers (i.e., their number and location), and the expansion of the wavefunction itself, which is not unique. The DMA sites are usually chosen to be the nuclei and the midpoint of covalent bonds. Out of this expansion local properties can be obtained such as the monopole and dipolar terms that are associated with each atom.

Both AIM and DMA are reasonable starting points for the construction of a continuum model of solvent effects in proteins based on the theory of polar liquids. To illustrate the approach proposed in this paper, DMA will be used to obtain the expansion of Eq. (3) and the energetics of a simple system, namely, the alanine dipeptide. A complete formalism for calculations of protein energetics based on AIM theory will be reported elsewhere.

LORENTZ–DEBYE–SACK–ONSAGER THEORY OF POLAR FLUIDS

Consider a point charge or dipole immersed in a solvent composed of molecules with isotropic polarizabilities α and permanent dipole moments $\boldsymbol{\mu}$. Regardless of its nature, the solute creates a field that orients and polarizes the surrounding molecules of the solvent. The polarization $\mathbf{P}(\mathbf{r})$ at a position $\mathbf{r}$ in the solvent is given by $\nu\mathbf{P}(\mathbf{r}) = \alpha\mathbf{E}_l(\mathbf{r}) + \langle f(\boldsymbol{\Omega})\rangle$, where $\mathbf{E}_l(\mathbf{r})$ is the local electric field related to the macroscopic (Maxwell) field $\mathbf{E}(\mathbf{r})$ by $\mathbf{E}_l(\mathbf{r}) = \mathbf{E}(\mathbf{r}) + (4\pi/3)\mathbf{P}(\mathbf{r})$; ν is the molecular volume of the solvent, and $\langle f(\boldsymbol{\Omega})\rangle$ is the Boltzmann average of the orientation-dependent function of the solute–solvent interaction energy w. Using the basic definition of electric displacement $\mathbf{D}(\mathbf{r}) = \mathbf{E}(\mathbf{r}) + 4\pi\mathbf{P}(\mathbf{r})$ and the Lorentz relationship between local and macroscopic fields, that is, $3\mathbf{E}_l(\mathbf{r}) = [\varepsilon(\mathbf{r}) + 2]\mathbf{E}(\mathbf{r})$, where $\varepsilon(\mathbf{r})$ is the dielectric permittivity, expressions for $\mathbf{E}(\mathbf{r})$ and $\mathbf{D}(\mathbf{r})$ can be obtained as a function of $\mathbf{E}_l(\mathbf{r})$ and the orienting field using the Debye–Sack approach, that is,

$$\mathbf{E}(\mathbf{r}) = \mathbf{E}_l(\mathbf{r}) - \frac{4\pi}{3}\left[\frac{\alpha}{\nu}\mathbf{E}_l(\mathbf{r}) + \frac{\langle f(\boldsymbol{\Omega})\rangle}{\nu}\boldsymbol{\mu}\right] \quad (5)$$

$$\mathbf{D}(\mathbf{r}) = \mathbf{E}_l(\mathbf{r}) + \frac{8\pi}{3}\left[\frac{\alpha}{\nu}\mathbf{E}_l(\mathbf{r}) + \frac{\langle f(\boldsymbol{\Omega})\rangle}{\nu}\boldsymbol{\mu}\right] \quad (6)$$

For an ionic source with charge q the orienting function is given by $f(\boldsymbol{\Omega}) = f(\theta) = \cos\theta$, where θ is the angle formed by vectors $\mathbf{r}$ and $\boldsymbol{\mu}$. The ion–dipole interaction energy is given by $w = -\mu E_l(\mathbf{r})\cos\theta$, thus $\langle f(\boldsymbol{\Omega})\rangle = \langle\cos\theta\rangle = L(\mu E_l(\mathbf{r})/kT)$, where k is the Boltzmann constant and $L(x) = \coth(x) - 1/x$ is the Langevin function. Using the linear approximation $\mathbf{D}(\mathbf{r}) = \varepsilon(\mathbf{r})\mathbf{E}(\mathbf{r})$ (i.e., nonlinear effects neglected) and $\mathbf{E}(\mathbf{r}) = q\mathbf{r}/\varepsilon(\mathbf{r})r^3$, an equation for $\varepsilon(\mathbf{r})$ is obtained from the above equations that depends on the distance r to the source [47, 48], namely,

$$\varepsilon(\mathbf{r}) = \varepsilon(r) = 1 + \frac{4\pi}{3}[\varepsilon(r) + 2]\frac{\alpha}{\nu} + \frac{4\pi\mu}{q\nu}r^2\varepsilon(r)L\left[\frac{q\mu[\varepsilon(r) + 2]}{3kTr^2\varepsilon(r)}\right]. \quad (7)$$

This equation describes the dielectric properties of a liquid in the presence of a point charge as derived from the LDS approximation (see a review in Ref. [49]). Iterative or numerical solutions of this equation yield dielectric functions of the sigmoidal form [33] (see below). For pure solvent the dielectric function $\varepsilon(r)$ is expressed in terms of measurable quantities only. The Lorenz–Lorentz relationship connects the polarizability of the solvent molecules with the high-frequency (optical) dielectric constant ε_∞ through $\alpha/\nu = 3(\varepsilon_\infty - 1)/4\pi(\varepsilon_\infty + 2)$. Far from the source Eq. (7) describes the static dielectric permittivity of pure bulk solvent ε_s, so an expression for μ is obtained, namely, $\mu^2 = (27kT\nu/4\pi)(\varepsilon_s - \varepsilon_\infty)/(\varepsilon_s + 2)(\varepsilon_\infty + 2)$. This expression yields values

of μ that are too small when compared with the dipole moment of water molecules, even in the gas phase. This observation led to reaction field corrections [32] to the LDS theory proposed by Onsager, in which only part of the local field $\mathbf{E}_l(\mathbf{r})$, the so-called directing field $\mathbf{E}_d(\mathbf{r})$, is responsible for the orientational effects on the solvent molecules. Therefore, only $\mathbf{E}_d(\mathbf{r})$ is used for the calculation of the average $\langle f(\mathbf{\Omega})\rangle$. The directing field can be expressed in terms of the orienting factor itself in the form [50] $\mathbf{E}_d(\mathbf{r}) = \mathbf{E}_l(\mathbf{r}) - \mathbf{R}(\mathbf{r})\langle f(\mathbf{\Omega})\rangle$, where $\mathbf{R}(\mathbf{r})$ is the reaction field at position $\mathbf{r}$ in the liquid, given by

$$\mathbf{R}(\mathbf{r}) = \frac{4\pi}{3\nu}\frac{2(\varepsilon(\mathbf{r}) - \varepsilon_\infty)}{2\varepsilon(\mathbf{r}) + \varepsilon_\infty^2}\frac{(\varepsilon_\infty + 2)}{3}\boldsymbol{\mu}. \quad (8)$$

With reaction field corrections (LDSO theory) a modified expression for $\varepsilon(\mathbf{r})$ is obtained [48], that is,

$$\varepsilon(r) = 1 + \frac{4\pi}{3}[\varepsilon(r) + 2]\frac{\alpha}{\nu} + \frac{4\pi\mu}{q\nu}r^2\varepsilon(r)L\left[\frac{q\mu[\varepsilon(r) + 2]}{(3kT + \mu R(r))r^2\varepsilon(r)}\right], \quad (9)$$

where $R(r) \equiv |\mathbf{R}(r)|$.

When the source of the field is a point dipole an expression for $\varepsilon(\mathbf{r})$ similar to Eq. (9) can be obtained; an overview of the derivation is given below [48]. If $\boldsymbol{\mu}_s$ is the dipole moment of the source, the macroscopic field is given by $\mathbf{E}(\mathbf{r}) = [3(\boldsymbol{\mu}_s \cdot \mathbf{r})\mathbf{r} - (\mathbf{r} \cdot \mathbf{r})\boldsymbol{\mu}_s]/\varepsilon(\mathbf{r})r^5$ where $\mathbf{r}$ is the position of the center of $\boldsymbol{\mu}$ relative to the center of $\boldsymbol{\mu}_s$. At any given instant of time the interaction energy between the solvent and source dipoles $\boldsymbol{\mu}$ and $\boldsymbol{\mu}_s$ is given by $w = -\mu\mu_s r^{-3}(2\cos\gamma\cos\theta - \sin\gamma\sin\theta\cos\phi)$, where θ is the angle formed by vectors $\mathbf{r}$ and $\boldsymbol{\mu}$ ($\mathbf{r}\cdot\boldsymbol{\mu} = r\mu\cos\theta$), γ is the angle formed by vectors $\mathbf{r}$ and $\boldsymbol{\mu}_s$ ($\mathbf{r}\cdot\boldsymbol{\mu}_s = r\mu_s\cos\gamma$), and ϕ is the dihedral angle defined by the vectors $\boldsymbol{\mu}$ and $\boldsymbol{\mu}_s$, and vector $\mathbf{r}$ that connects their centers, as the reference. In this case the calculation of $\langle f(\mathbf{\Omega})\rangle$ is not straightforward and a general analytical solution is difficult to obtain. Under the approximation of small dipole fields an expression is obtained as $\langle f(\mathbf{\Omega})\rangle = 2\cos\gamma\, L(\mu E_l(\mathbf{r})/kT)$. For a given spatial orientation of $\boldsymbol{\mu}_s$ the spherical symmetry that led to Eqs. (7) and (9) is now broken and $\varepsilon(\mathbf{r})$ depends on the position $\mathbf{r}$ in the solvent and not only on the distance r to the point source [48]. However, a second Boltzmann average can be taken on all orientations of the source dipole (i.e., on all possible angles γ), thus recovering the spherical symmetry of the dielectric profile. In this case an expression analogous to Eq. (9) above is obtained, namely,

$$\varepsilon(\mathbf{r}) = \varepsilon(r) = 1 + \frac{4\pi}{3}[\varepsilon(r) + 2]\frac{\alpha}{\nu} + \frac{2\pi\mu}{\mu_s\nu}r^3\varepsilon(r)L\left[\frac{2\mu\mu_s[\varepsilon(r) + 2]}{(3kT + \mu R(r))r^3\varepsilon(r)}\right], \quad (10)$$

where the reaction field $R(r)$ is the same as above (the reaction field of the source is neglected in its local orienting field for calculating the second average). Equation (10) is mathematically similar to Eq. (9), and the dielectric functions obtained from both equations exhibit sigmoidal behavior with the distance r.

Continuum Electrostatics Based on Screened Coulomb Potentials

For a source point charge q in a dielectric medium it is always possible to define a screening function $D(\mathbf{r})$ such that the electric potential at position $\mathbf{r}$ can be expressed as $\phi(\mathbf{r}) = q/D(\mathbf{r})r$. The relationship between the physically measurable dielectric function $\varepsilon(\mathbf{r})$ and the screening function $D(\mathbf{r})$ is found from the definition $\mathbf{E}(\mathbf{r}) = -\nabla\phi(\mathbf{r})$. For a point charge this relationship is given by

$$\varepsilon(r) = D(r)\left[1 + \frac{r}{D(r)}\frac{d}{dr}D(r)\right]^{-1}. \quad (11)$$

Once the dielectric function $\varepsilon(r)$ is known from theoretical considerations, for example, the LDSO theory [cf. Eq. (9)], or experimental measurements, $D(r)$ can be evaluated from Eq. (11) (see below). Both $\varepsilon(r)$ and $D(r)$ are sigmoidal functions and approaches the same asymptotic value as r increases [33].

It may already be noticed that a continuum formulation based on the LDS theory can be directly related to atomic properties of the molecule, that is, local charges, Q, and local dipoles, $\boldsymbol{\mu}_s$, which in turn may be obtained using approximate quantum chemical calculations. This procedure formally links the screening functions $D(\mathbf{r})$ with the molecular electron density obtained from ab initio calculations. A continuum approximation based on screening potentials for use in peptides and proteins has been reported [33–36] and an overview of the approach is given below. The model, dubbed "SCP

continuum model," is based on $D(\mathbf{r})$, not on $\varepsilon(\mathbf{r})$, and the precise form of $D(\mathbf{r})$ is determined from the parameterization of the model as reported elsewhere [33, 34, 51].

Formally, once $\varepsilon(r)$ is known, for example, from Eq. (9), inversion of Eq. (11) can be carried out by numerical integration to obtain $D(r)$. From a practical point of view, however, it is useful to invert it analytically. A first-order differential equation with sigmoidal solutions is sufficient and was proposed earlier [52], namely,

$$\frac{dD(r)}{dr} = \lambda(1 + D(r))(D_s - D(r)), \qquad (12)$$

where D_s has the value of the bulk dielectric constant and λ controls the rate of increase of $D(r)$. Introducing Eq. (12) into Eq. (11) yields a quadratic form in $D(r)$ that can be solved as an explicit function of r and $\varepsilon(r)$. A solution of Eq. (12) is given by

$$D(r) = (1 + D_s)/[1 + k\exp(-\alpha r)] - 1, \qquad (13)$$

where k is a constant of integration and $\alpha = \lambda(1 + D_s)$. It is seen that the physics of the system [Q, μ, μ_s, ε_∞, etc, i.e., the quantities that define $\varepsilon(r)$ in Eq. (9)] is contained in the parameter λ (or α), and this can be calculated from experimental data in the limit of simple systems. Moreover, this particular sigmoidal form of $\varepsilon(r)$ or $D(r)$, i.e., solutions of Eq. (12), allows a good fit of the screening obtained from experimental data. Note that because λ (or α) depends, in particular, on atomic charges and dipoles of the solute and can be obtained from the LDSO theory, it is possible to derive a first-order, parameter-free continuum model of solvation by combining quantum chemistry and classic theory of liquids. This procedure is formally proposed herein.

For a system composed of N charges q_i the potential can be expressed in the general form

$$\phi(\mathbf{r}) = \sum_{i=1}^{N} \frac{q_i}{D(\mathbf{r})|\mathbf{r} - \mathbf{r}_i|} \qquad (14)$$

at any arbitrary point $\mathbf{r}$; here it is assumed that $D(\mathbf{r})$ and $\varepsilon(\mathbf{r})$ are scalar functions. The exact form of $D(\mathbf{r})$ in Eq. (14) is not known in general and is one of the fundamental questions in molecular electrostatics. The simplifying approximation made for deriving the SCP is to assume that $D(\mathbf{r})$ can be expressed in terms of distance-dependent screening functions $D_s(|\mathbf{r} - \mathbf{r}_i|)$ centered at each atom coordinate $\mathbf{r}_i$. In this case the potential is expressed as a superposition of the form (index s stands for "solvent" following previous notation)

$$\phi(\mathbf{r}) = \sum_{i=1}^{N} \frac{q_i}{D_s(|\mathbf{r} - \mathbf{r}_i|)|\mathbf{r} - \mathbf{r}_i|} \qquad (15)$$

and, then, the *position*-dependent screening function $D(\mathbf{r})$ is formally given in terms of the *distance*-dependent screening functions by $D(\mathbf{r}) = \Sigma_i\, q_i/|\mathbf{r} - \mathbf{r}_i|/\Sigma_i\, q_i/|\mathbf{r} - \mathbf{r}_i|D_s(|\mathbf{r} - \mathbf{r}_i|)$. Note that $D(\mathbf{r})$ is a continuous function of the position (except at $\{\mathbf{r}_i\}$) and depends on the particular distribution of charges in the system, as expected.

From Eq. (15) and using a standard thermodynamic path an expression for the total electrostatic energy, U_T, of a molecule in the polar liquid is obtained [33, 34], which is given by

$$U_T = \frac{1}{2}\sum_{i\neq j}^{N} \frac{q_i q_j}{D_s(r_{ij})r_{ij}} + \frac{1}{2}\sum_{i=1}^{N} \frac{q_i^2}{R_{i,B}}\left[\frac{1}{D_s(R_{i,B})} - 1\right], \qquad (16)$$

where the first sum is the interaction term and the second, the self-energy contribution. In the context of a molecule, unlike an isolated particle considered above, $D_s(r)$ represents the screening function that accounts for all the screening mechanisms in the system around a given particle; $R_{i,B}$ is the effective Born radius of atom i in the solvated molecule.

Combining LDSO and DMA Approaches into the SCP Continuum Model

NUMERICAL CALCULATION OF DIELECTRIC AND SCREENING FUNCTIONS

Figure 1 shows the dielectric function $\varepsilon(r)$ and the associated screening function $D(r)$ for a point charge in water. Iterative solutions for other solvents were reported previously [33]; solutions of Eqs. (7) and (9) are symmetrical in Q. Here screening functions were obtained by a numerical integration of Eq. (11) with the condition that it reaches an asymptotic value as $r \to \infty$. The experimental data used to solve these equations were as follows: Q =

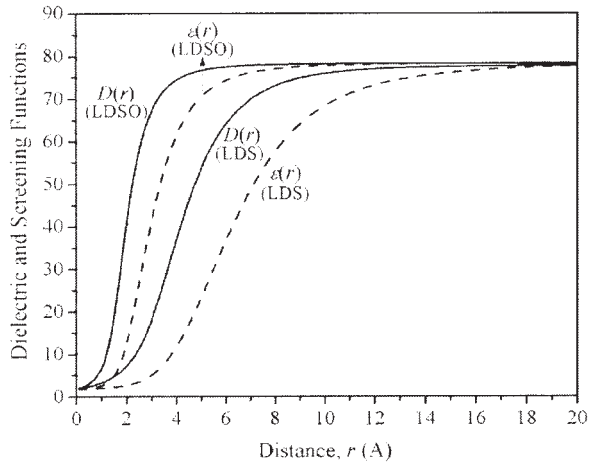

FIGURE 1. The LDS and LDSO dielectric profiles, $\varepsilon(r)$, and the corresponding screening functions, $D(r)$, induced by a point charge $Q = e$ in water ($T = 298$ K) as a function of the distance, r, to the source; $\varepsilon(r)$ were obtained numerically from Eq. (7) (LDS) and Eq. (9) (LDSO), whereas $D(r)$ were obtained by numerical integration of Eq. (11).

e, $\mu = 0.82$ D, $\varepsilon_s = 78.39$, $\varepsilon_\infty = 1.78$, $\nu = 29.8$ Å^3, $T = 298$ K; with these values the polarizability α can be obtained from the Lorenz–Lorentz relationship. The dielectric function $\varepsilon(r)$ shows a smooth increase with the distance and reaches the bulk solvent value at $r > 15$ Å (LDS) or $r > 7$ Å (LDSO). The screening functions $D(r)$ are steeper than $\varepsilon(r)$ and reach their asymptotic values at shorter distances from the central charge, that is, at $r > 11$ Å (LDS) or $r > 5$ Å (LDSO). The effect of the reaction field corrections is to shift the profile toward smaller values of r. As a general rule the larger is the charge Q, the lower is the slope of $\varepsilon(r)$ within the changing region. This is clearly observed in Figure 2(a), which displays $\varepsilon(r)$ (LDSO) for different values of the point charge $Q = Ze$. Figure 2(b) shows the corresponding screening functions, $D(r)$, obtained from a numerical integration of Eq. (11). The range of charges covers all values obtained from a partitioning of the molecular electron density; in particular it includes partial charges as defined in standard molecular mechanics force fields for macromolecules. Table I shows the monopoles and dipole moments obtained from a DMA analysis of the minimized structures of the N-acetyl-L-Alanine-N-methylamide (atom names follows CHARMM nomenclature). The calculations were carried out using density functional theory (DFT) with a gradient-corrected three parameter B3LYP exchange-correlation functional [73, 74], and the 6-31G* basis set. Figure 3 shows $\varepsilon(r)$ (LDS with $Q = e$) and two additional $D(r)$ curves, one calculated numerically from the definition [cf. Eq. (11)] and a second one from the proposed differential equation [cf. Eq. (12)]; the experimental conditions are as in Figure 1. For the value $\lambda = 0.011$ Å^{-1} ($\alpha = 0.87$ Å^{-1}) a good fit to the exact $D(r)$ [cf. Eq. (11)] is obtained at all distances, which deteriorates only at the shoulder of the curve. However, because of the large value of $D(r)$ in this region, the difference in the interaction energy calculated from these two curves is negligible. For a set of experimental con-

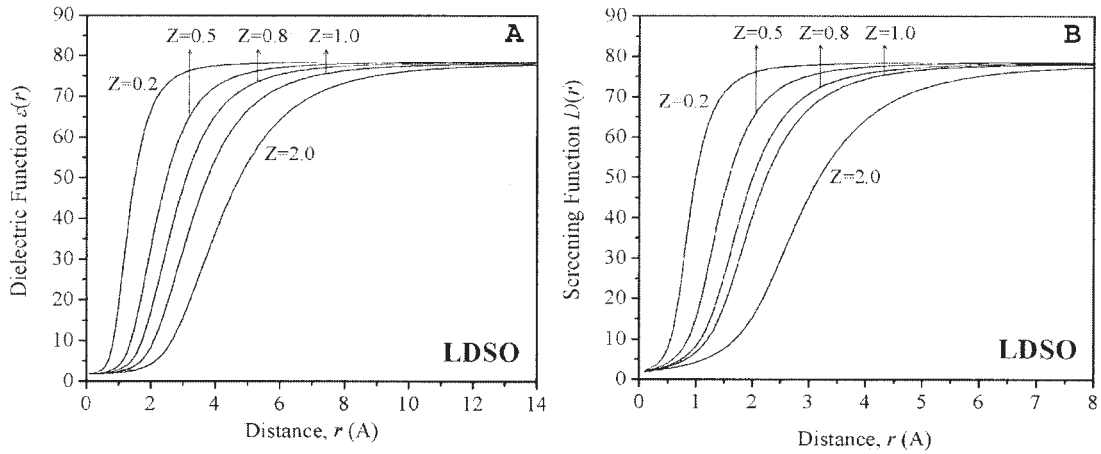

FIGURE 2. (a) Dielectric and (b) screening functions in water induced by a representative set of point charges $Q = Ze$ as a function of the distance, r, to the source, at $T = 298$ K; $\varepsilon(r)$ and $D(r)$ were obtained numerically from Eqs. (9) and (11), respectively (LDSO theory).

TABLE I

Monopole and dipole components of a DMA of N-acetyl-L-Alanine-N-methylamide.[a]

Atom	Charge, Q	Dipole moment, μ
CAY	−0.218	0.043
HY1	0.028	0.165
HY2	0.076	0.164
HY3	0.078	0.166
CY	0.956	0.305
OY	−0.887	0.325
N	−0.689	0.248
HN	0.332	0.064
CA	0.171	0.514
HA	0.035	0.166
CB	−0.115	0.217
HB1	0.028	0.160
HB2	0.053	0.165
HB3	0.067	0.164
C	0.985	0.354
O	−0.870	0.330
NT	−0.725	0.208
HNT	0.400	0.091
CAT	0.150	0.511
HT1	0.032	0.162
HT2	0.040	0.163
HT3	0.073	0.170

[a] Charges Q are given in fractions of e and dipole moments μ in Debye. Atom names follow CHARMM force-field nomenclature.

ditions (and a given solvent) a value of λ can be obtained that fits $D(r)$ of Eq. (12) to the form of Eq. (11). At a given temperature a curve $\lambda(Q)$ can be obtained as shown in Figure 4, which has an exponential-decay type behavior. Similar curves can be obtained for a point dipole, but this case is not considered here. Suffice it to say that for a dipolar source, the qualitative behavior of $\varepsilon(r)$ is similar to the case of an ion, but the increase of $\varepsilon(r)$ with the distance is faster than shown in Figure 1 [48].

DETERMINATION OF PARAMETERS AND PARAMETER MISMATCH

Equation (16) has been used in a number of problems involving peptides and proteins [33–36, 53, 54]. To be useful, the parameters α in the screening functions D_s had to be derived first. Chemical atom-type parameters were optimized by fitting experimental solvation energies of amino acid side chain analogs [33]. This illustrates one of the drawbacks of MM approximations over *ab initio* QM,

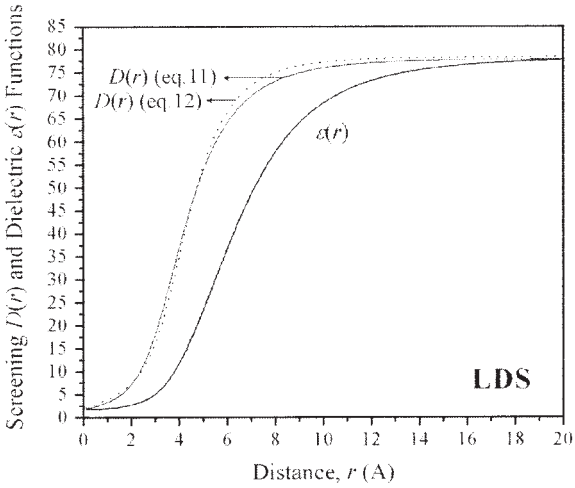

FIGURE 3. Distance dependence of the dielectric function $\varepsilon(r)$ obtained from the LDS theory for a point charge $Q = e$ [cf. Eq. (7)] and the corresponding screening functions $D(r)$ obtained from a numerical integration of Eq. (11) (solid line), and as a solution of the quadratic form obtained by introducing Eq. (12) [with solutions given by Eq. (13); see text] into Eq. (11) (dotted line): $Q = e$ ($Z = 1$), $\varepsilon_s = 78.4$, $\varepsilon_\infty = 1.78$, $T = 298$ K.

namely, the need to define empirical parameters prior to carrying out calculations. As discussed above, continuum models for use in macromolecular systems vary broadly in the way the potential function is defined and in the parameter definitions. The procedure reported in this paper aims at

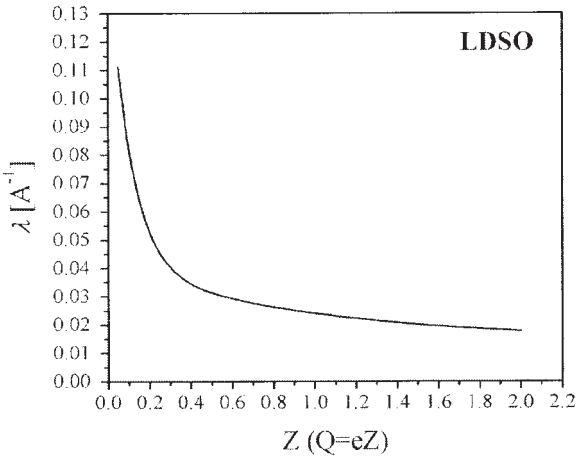

FIGURE 4. Dependence of the parameter $\lambda(Q)$ in the first-order differential equation for $D(r)$ [cf. Eq. (12)] with the charge $Q = Ze$ of the source (LDSO theory).

minimizing this limitation in a continuum model of solvation, in particular in the SCP-based model described earlier [33–35].

Another difficulty arising from the need to define parameters a *priori* in MM force fields is that it complicates comparing results obtained from different continuum methods. This occurs because it is often difficult to ensure that the parameters defining each of the models to be compared have been optimized to the same degree of accuracy or to assess the level of physical information contained in each model. Thus, the parameters defining each of the models to be compared may be mismatched. Because such parameter mismatch (PM) can have broader implications regarding the reliability of a particular model (as discussed in the introduction), some of its consequences are detailed in the following discussion. One form of the problem is well represented by the frequently used comparison of a mature approach, for example, the generalized Born (GB) continuum model [55] in any of its many forms with, say, linear dielectric screening in the form [56] $\varepsilon = ar$. In these analyses the mature models include at least the electrostatic interactions and the self-energy contributions. Moreover, the parameters have been carefully optimized by fitting results of Poisson–Boltzmann (PB) calculations (see below) or experimental results such as solvation energies. In contrast, no or little optimization has been done for the general linear term $\varepsilon = ar + b$. Instead b is arbitrarily set to zero and a is often given the value 1 or 2. No justification is given for these values, and important parts of the physics of solvation (e.g., self-energy) are also lacking. Because of these defects the linear dielectric, for example, $\varepsilon = 2r$, performs poorly in comparison with an optimized model in describing the electrostatics of solvation. Better parameterization of the linear form was suggested earlier, for example, the form [57] $D(r) = 4.5r$ and the optimized form, $D(r) = 6.7r - 8.57$, had been proposed [58] by fitting to Eq. (13). However, the reliability of these simple proposals has not been fully explored.

A recently proposed approach for the rapid calculation of solvation energies of proteins represents another example of PM in the comparison of two methods [59]. The method was designed to carry out fast calculations of the Born radii, R_i, that appear in the interaction term of the GB model (i.e., the terms containing the quantity $(R_iR_j)^{1/2}$). The authors intended to use their approach in the context of a GB-like formulation. The approach consisted in first dividing all pair interactions into three classes: 1–2 (between covalent-bonded atoms), 1–3 (between two atoms covalently bonded to a common atom), and the rest of the nonbonded interaction (1–4 and higher). It is noted, however, that MM force fields use only the last class to calculate nonbonded interaction energies. The authors used five parameters for each of these three classes, although for the 1–4 class three of the parameters were given preassigned values [59]. Thus, the method proposed used a set of 15 parameters, 12 of which were optimized by fitting pair interaction energies to the corresponding values obtained from solution of the Poisson equation. In the optimization of their method the authors used a set of over 50 proteins that were also used for all the subsequent comparisons. The proteins ranged in size from ~10 to ~110 amino acids. For all the PB calculations and optimization the authors assigned the same internal dielectric constant of $\varepsilon_i = 2$ to all the proteins of the set. In addition, the same probe radius and external dielectric constant were used (see Ref. [59]).

The authors compared their method with a distance-dependent screening function similar to Eq. (13), given by $D(r) = A + B/(1 + a\exp(-br))$. Here a and b are the two parameters that were optimized (A and B were chosen such that $D(0) = 1$ and $D(\infty) = \varepsilon_s$). The details of the procedure used to optimize these two parameters are given in Ref. [59]. In the optimization of $D(r)$, apparently all three classes of interactions (i.e., 1–2, 1–3, and 1–4 and larger) were taken together to obtain the values of a and b. However, the three classes had been optimized separately, three sets of the parameter pairs, a and b, would have been obtained. The drawback of the approach used by the authors to optimize $D(r)$ is that it leads to an extremely distorted form of the screening function because the fitting will naturally emphasize the largest values of the target function (1–2 and 1–3 pair interactions in this case). This can be seen in Figure 5, where $D(r)$ using the reported values of a and b is plotted (D_{HMWC}) along with the form proposed originally [52] for the SCP (D_{WDS}). It is clear that D_{HMWC} is very different from D_{WDS}, and for distances $r < 10$ Å D_{HMWC} strongly underscreens all electrostatic interactions. That such PM can lead to artifactual results can be seen from an earlier comparison of pair energies calculated with D_{WDS} and with the original version of the GB [55]. The scatter plot of these energies (Fig. 4 in Ref. [60]) showed a good agreement between the two methods, in contrast to the findings in Ref. [59]. The reason for this is that the effective screen-

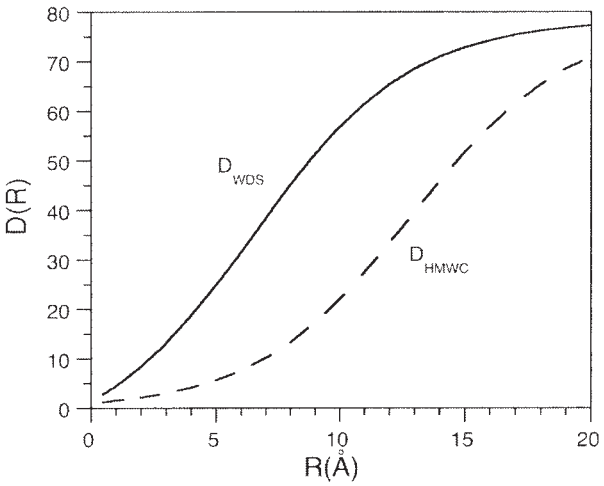

FIGURE 5. Screening functions calculated from different parameterizations: $D_{wds}(r)$ (as reported in Ref. [60]) and $D_{HMWC}(r)$ (as reported in Ref. [59]).

ing in the GB was essentially the same as that provided by D_{WDS} (see Fig. 3 in Ref. [60]).

In the previous sections the form of $D(r)$ was derived from basic electrostatic considerations, and previous works have demonstrated that methods yielding reasonable results screen the interactions in a way that closely resembles $D(r)$, including PB-derived screening [61]. Therefore, it is not surprising that interaction energies calculated with D_{HMWC} do not compare well with GB or PB results because of the mismatch in parameters.

Another fundamental problem related to the discussion above is the nature of the target function used for parameter optimization. It is customary to use results from PB calculations as the standard for fitting and parameter optimization of some solvation models. Such a procedure is reasonable because of the fundamental nature of the Poisson equation and the rigorous statistical arguments that leads to the nonlinear PB equation. Because the PB equation can be solved only numerically when applied to macromolecules, it is necessary to make a number of *a priori* assumptions when the PB method is used to calculate electrostatic properties. The most basic assumptions consist in assigning values to the internal, ε_i, and external dielectric constant, ε_s, and to define a location of the solvent/solute boundary, i.e., to define a probe radius r_p. These assumptions are problematic because it is known that the values assigned to ε_i, and r_p, although reasonable, are arbitrary. In proteins typical values used are in the range of $\varepsilon_i = 1$–4, $\varepsilon_s = 80$, and $r_p = 0$–1.4 Å, although other values have also been used. It is known that numerical solutions of the PB equation may be very sensitive to small changes of these values [62] (see below). Proteins are nonhomogeneous systems whose internal dielectric values are not well defined, and to represent the inhomogeneity, different values of ε_i have been assigned to different regions of the same protein. Moreover, as discussed above, it is not straightforward to define a sharp solute/solvent boundary, because dielectric profiles in polar liquids vary smoothly with the distance. This freedom of choice may introduce a high degree of arbitrariness that is transferred to the parameters of a solvation model if simplistic PB results are used in its parameterization.

The problem is quantitatively illustrated in the scatter plot of Figure 6, which shows per-atom solvation energies in a wild-type domain of Barnase, a 110 amino acid protein (pdb code: 1a2p). These solvation energies were calculated with the UHBD PB solver [63] using two sets of ε_i and r_p values: $\varepsilon_i = 1$ and $r_p = 0$ Å; and $\varepsilon_i = 4$ and $r_p = 1.4$ Å ($\varepsilon_s = 80$ for both cases). Most of the calculations in protein electrostatics use values between these two limits. Protein 1a2p is the largest molecule in the set of 50-plus proteins used in Ref. [59] and discussed above (coordinates kindly provided by the authors). The solvation energy of a given atom i is calculated as the solvation energy of the whole

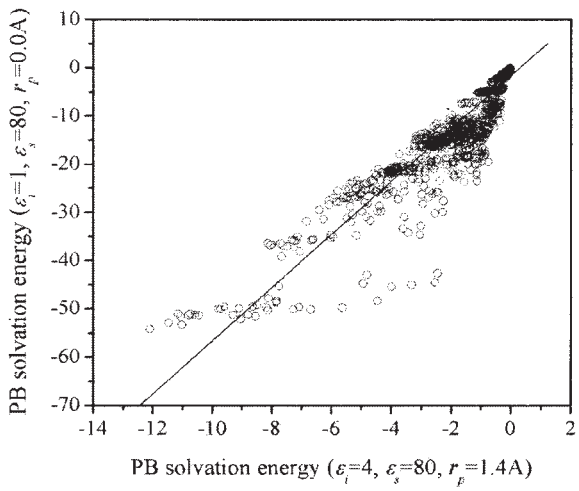

FIGURE 6. Scatter plot of atomic solvation energies in Barnase (pdb code: 1a2p) for two sets of (ε_i, ε_s, r_p) values (units in kcal/mol), at zero ionic strength calculated from the PB equation; the PB solver in the UHBD [63] program was used (see text).

protein when all charges ($q_j \; \forall j \neq i$) are set to zero, except the partial charge q_i of atom i. The range of solvation energies changes from 12 kcal/mol for $\varepsilon_i = 4$, $r_p = 1.4$ Å to about 55 kcal/mol for $\varepsilon_i = 1$, $r_p = 0$ Å. Both the slope and the correlation (the straight line is a linear fit) are strongly shifted from the ideal (or desirable) value of one. More important than the slope of the correlation is the large number of outliers observed: atoms that display the largest differences in energies with respect to the straight line (in some cases about 30 kcal/mol) belong to exposed side chains in the protein. As a rule the larger is the charge of an atom, the larger is the difference in the calculated energy. This is very unfortunate because charged groups are at the same time more frequently found on the protein surface. These exposed groups are also involved in interactions and binding with other proteins and ligands; thus, large errors in their solvation energies may render the quantitative interpretation of a calculation meaningless. In fact, the differences in energies observed in Figure 6 are unacceptable in biological systems because errors on the order of $RT = 0.6$ kcal/mol (room temperature) may already have an important effect in the calculation of both structure and dynamical properties, hence, on thermodynamic quantities. In contrast to exposed charged groups, deeply buried groups are mostly insensitive to changes in ε_i and r_p, and the smaller is the charge of the atom, the smaller are the errors in energy. Actually, buried uncharged groups contribute the most to the positive correlation observed in Figure 6, especially in the region of small solvation energies.

From the discussion above a question emerges as to what set of values (i.e., ε_i, ε_s, and r_p) should be used in these simple PB calculations when optimizing parameters of a solvation model. In Ref. [59] all the proteins of the set were assigned the same values of ε_i, ε_s, and r_p, but any value in the range considered in Figure 6 could have been chosen, or even different sets of values for different proteins. Moreover, the LDS theory shows that the rate of increase of $\varepsilon(r)$ with the distance depends on the atoms, so an atom-dependent r_p would be more reasonable if a sharp boundary is to be defined in the calculations.

It is clear, then, that to be able to reliably apply a particular methodology to systems that may show large variability in size scale, environment, and chemical nature, a more rigorous approach is needed to minimize empiricism and arbitrary assumptions. It is proposed here that parameters developed for use in continuum models of solvent effects should ideally include the following properties: *(i) to have a clear connection with physical quantities and experimental control variables (e.g., temperature and ion concentration); (ii) converge to quantities that can be calculated from experimental data in the limit of simple systems; and (iii) to be transferable between molecular systems.* These basic guidelines, which are interrelated, would probably help to bridge the QM–MM gap discussed in the Introduction and form the basis of a more general model for use in molecular systems of varying size scales. The implementation outlined here is a first attempt to follow these guidelines in a more systematic way than previously pursued in the context of the SCP-ISM for macromolecules.

For small molecules the LDSO theory and the DMA or AIM methods can be combined self-consistently for the *ab initio* calculation of molecular structure in solution. Thus, an initial set of charges $\{q_{i,0}\}_{i=1,N}$ is obtained from a DMA analysis in vacuum (e.g., as in Table I for alanine dipeptide). These charges are used to obtain atom-dependent screening $\{D_{i,0}(r_i)\}_{i=1,N}$ centered at the coordinates of each nucleus, $\{\mathbf{r}_i\}_{i=1,N}$. For this assignment the plot of Figure 4 is used, which is independent of the nature of the molecule, although the molecular structure is implicit in the charge distribution. With this vacuum-based set of screening functions a new set of charges is obtained from the new optimized molecular structure. The new charges are then fed back to the plot of Figure 4 and a new set of screening parameters is obtained. The procedure is repeated until convergence is attained. Note that a similar self-consistent procedure was reported earlier for another method [19, 64]. This procedure, valid in the context of a pure QM calculation is not described here.

A simplified but more practical implementation for use in macromolecules can be used for calculations in the context of a MM force field as described below. The main advantage of this procedure is that the properties (i) and (ii) suggested above are naturally satisfied, whereas directions are discussed to attain point (iii) with the help of AIM theory. The main idea is to use the partial charges of the force field or from an *ab initio* method and to derive the correct value of the parameters from Figure 4. After a set of charges is available, Eq. (16) is used to calculate the electrostatic component of the total molecular energy of the MM force field as previously discussed [33, 34] (see also URL at Ref. [65]). The key issue of this procedure is that it does not

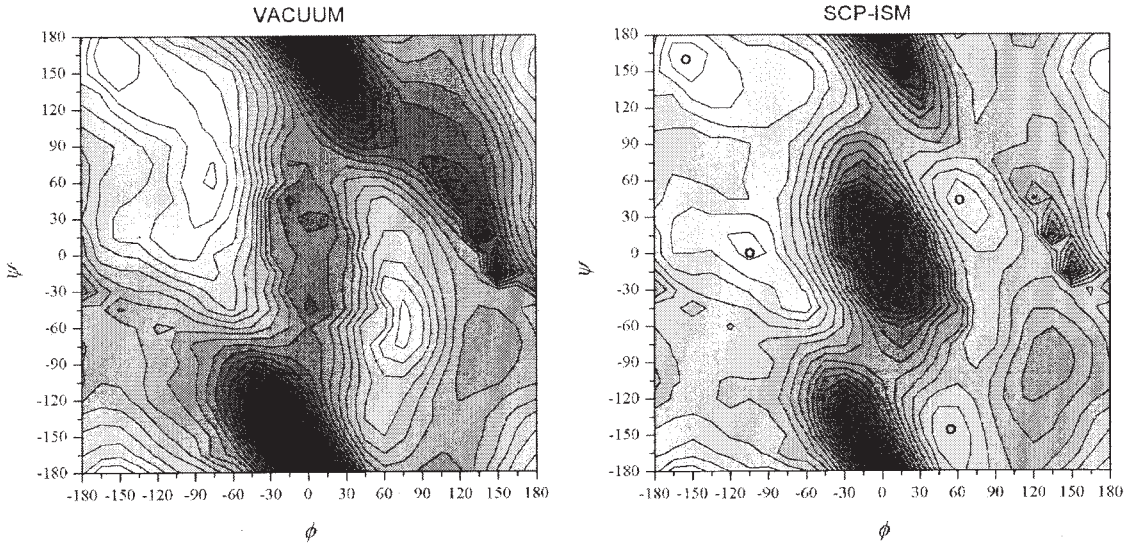

FIGURE 7. (Free) energy surface (Ramachandran plot) of the alanine dipeptide using the CHARMM/CMAP force field in vacuum (left panel) and with the SCP-ISM (right panel). Details of the calculation are reported in Ref. [35] (see also URL at Ref. [65]) with screening parameters obtained from Figure 4. Atomic charges were obtained from the PAR22 all-atom parameters of the CHARMM force field (c31b1 version). Contour plots are at increments of 1 kcal/mol in both panels and the lowest energy corresponds to the C_7^{eq} conformation (see Discussion in Ref. [34]).

require a parameterization of the solvent model in the usual (*a priori*) sense, so any new molecule can be studied as long as a set of charges (and possibly dipoles) is defined. This is particularly useful for small molecules in the context of a MM calculation. It is also useful for proposing an initial condition for further refinement based on self-consistency of the kind mentioned above or as the reference for a perturbative approach. Also fundamental is that the method would allow a great amount of flexibility if a polarizable MM force field is used to describe the solute because the parameters of the continuum model would adjust themselves in a predicted way to the fluctuating charges and dipoles in the molecule.

Figure 7(left panel) shows the in-vacuum energy surface of the alanine dipeptide calculated using the CHARMM force field (c31b1 version) with the recently developed CMAP dihedral potential [66]. The calculation was carried out as described in a previous publication [34]. This CHARMM/CMAP combination along with the SCP-based continuum model (SCP-ISM) was shown to reproduce structural and dynamic properties of proteins in long dynamics calculations [35, 36, 67]. Figure 7(right panel) displays the energy surface modified by the solvent using Eq. (16) and parameters obtained from Figure 4 using PAR22 charges [14]. Contours are plotted at 1 kcal/mol increments from the global minimum (C_7^{eq}). It is interesting to compare the SCP-ISM/CHARMM/CMAP surface of Figure 7(right panel) with Figure 6 in Ref. [10] and also Figures 1 and 2 in Ref. [66]. The positions of the minima [cf. Table II] are in qualitative agreement with previous QM/MM calculations as well as with statistical distributions obtained from a search in the Protein Data Bank. The relative energies and positions of the minima in the plot of Figure 7(right panel) are shown in Table II. There are four well-defined minima corresponding to the C_7^{eq}, C_7^{ax}, α_R, and α_L and discussed in previous publications, although the positions and relative energies have changed, as expected. The most dramatic change is

TABLE II

Position and energy of the minima of the energy surface of the alanine dipeptide in the (ϕ, ψ)-space (error estimated from the grid spacing used in the calculations).

	C_7^{eq}	C_7^{ax}	α_R	α_L
Energy (Kcal/mol)	0.0	3.7	1.1	2.7
(ϕ, ψ) ± 3°	(−154, 160)	(55, −154)	(−104, 0)	(61, 44)

observed in the energy of the α_L minimum that drops from about 7.8 kcal/mol with the SCP-ISM/CHARMM/PAR22 to about 2.7 kcal/mol in the new implementation [66]. Interestingly, the energy surface calculated with the SCP-ISM as implemented into the c31b1 version of the CHARMM force field, when used with the CMAP potential, yields results quantitatively similar to those reported above [36]. It is noted that incorporation of a simple hydrophobic term proportional to the solvent-accessible surface area does not change the results beyond the expected uncertainty of the calculations [36].

Conclusions

In this paper an approach is proposed for incorporating a solvent continuum model into microscopic (QM), macroscopic (MM), and hybrid (QM/MM) algorithms for calculating macromolecular structure and properties of macromolecules. The basis of the method is the multicenter-multipole expansion of the electrostatic potential of a solute molecule that leads to a local description of charge and dipole moment. While such partitioning is not unique, it can be based on reasonable mathematical or physical arguments as exemplified by the AIM method developed by Bader et al. [21–25] or Stone's DMA approach [26, 27]. When the system is immersed in a continuum solvent, its potential can be written in the form of Eq. (14), and introducing the approximation that the position-dependent $D(\mathbf{r})$ can be expressed in terms of distance-dependent screening functions, an expression for the total potential $\phi(\mathbf{r})$ in terms of atom-centered contributions $\{\phi(\mathbf{r} - \mathbf{r}_i)\}_{i=1,N}$ is recovered that can be formally related to Eq. (2).

In the unified approach suggested here, the necessity for the *a priori* determination of the parameters defining the continuum model that is incorporated into the MM force field can be replaced by a self-consistent approach. This approach is illustrated in Figure 4, which shows that the optimal values of λ [cf. Eq. (12)] depends on the charge, Q, at a given temperature. A similar plot can be obtained as a function of the magnitude of the dipole moment μ. As shown in the example, given a particular force field, the λ can be determined directly from Figure 4. The procedure was applied to the alanine dipeptide, and the results show good agreement with QM/MM calculations [10, 66]. Circumventing the need for the *a priori* determination of parameters for a particular continuum model avoids the type of PM discussed in the fourth section. These include the PM between two approaches that are to be compared, and the PM that might occur when parameters are fit to results from other theoretical methods, such as the PB equation. As shown in the scatter plot of Figure 6, the values of the calculated interaction energies are very sensitive to the values of ε_i and r_p used in the calculation. In particular, the interaction energies calculated from larger charge values are poorly correlated. This sensitivity will certainly be reflected in the values of the fitted parameters and may lead to severe distortion when the continuum model is applied to real systems (for which ε_i and r_p are not known).

The approach proposed herein also has implications if polarizable MM force fields are considered. In these cases, the dielectric properties of the system are expected to change in response to the local dipole and charge distribution. If parameters are obtained from fixed electronic structure, as is the case in the majority of the continuum models used in MM force fields for biomolecules, this adaptation is not possible. The simple law displayed in Figure 4 that is followed by the parameter $\lambda(Q)$ versus Q (this numerical curve can be fitted accurately by the sum of two simple exponential-decay functions) can be further generalized to include the effects of the dipole moment, namely, $\lambda(Q, \mu)$. This expression of λ as a function of Q and μ makes it possible to carry out "on the fly" recalculation of the position-dependent screening. The adaptation of the screening to fluctuating local charges and dipoles in the solute offers a desirable flexibility that is lacking in most continuum models of solvation in MM force fields.

It is clear from the above discussion that a "parameter-free" continuum model is a desirable goal and the procedure proposed in this paper is an initial step in this direction. A complete formalism for computer simulations of polymers and other mesoscopic systems will be reported elsewhere. The method of determining the function $\lambda(Q)$, shown in Figure 4, clearly conforms to conditions *(i)* and *(ii)* discussed in the last section, but its transferability (condition iii) still needs to be established. The original *a priori* determination of the parameters [33, 35] of the SCP-ISM (i.e., the λ or α) have implicitly been assumed to be transferable, an assumption that appears to be reasonable in view of the successful results obtained in many standard tests in proteins and peptides. However, as dis-

cussed elsewhere [34], many of these tests would be inadequate to assess the quality of a continuum approximation. For this reason it is also expected that the possibility of studying small molecules at the QM level using the multicenter-multipole-LDSO–based SCP approach described here would offer more stringent tests for the quality of the continuum approach. Calculations that seem relevant for this task are the study of the effect of the solvent on the conformations and vibrational and electronic spectra of small molecules, in addition to comparisons with experimental data.

Finally, it is worthwhile to keep in mind that a continuum approximation cannot describe all the physics of solvation, as discussed in Refs. [35, 36]. In particular, hydrophobicity [68–71], hydrogen-bonding interactions [51, 72] and, possibly, the local granularity of the liquid around exposed atoms are important physical effects that must be considered when studying dynamic properties of biomolecules.

ACKNOWLEDGMENTS

Computational support was provided by the National Science Foundation Terascale Computing System at the Pittsburgh Supercomputing Center, by the Advanced Scientific Computing Laboratory at the Frederick Cancer Research Facility of the National Cancer Institute (Laboratory of Mathematical Biology), and the high-performance computational facility of the Beowulf PC/Linux cluster at the National Institutes of Health, Department of Health and Human Services, Bethesda, Maryland (http://biowulf.nih.gov). The authors also acknowledge access to the computer facilities at the Institute of Computational Biomedicine (ICB) of Weill Medical College of Cornell University. Partial support of the work by NIH grant R01 DA15170 is gratefully acknowledged.

References

1. Tse, J. S. Annu Rev Phys Chem 2002, 53, 249–290.
2. Ben-Nun, M.; Martinez, T. J. In Advances in Chemical Physics, Volume 121; Prigogine, I.; Rice, S. A., Eds.; John Wiley: New York, 2002, 439–512.
3. Tuckerman, M. E. J Phys Condens Matt 2002, 14, R1297–R1355.
4. Carloni, P.; Rothlisberger, U.; Parrinello, M. Accounts Chem Res 2002, 35, 455–464.
5. Lee, Y. S.; Krauss, M. J Am Chem Soc 2004, 126, 2225–2230.
6. Khorana, H. G. J Biol Chem 1988, 263, 7439–7442.
7. Car, R.; Parrinello, M. Phys Rev Lett 1985, 55, 2471.
8. Parrinello, M. Solid State Commun 1997, 102, 107–120.
9. Geissler, P. L.; Dellago, C.; Chandler, D.; Hutter, J.; Parrinello, M. Science 2001, 291, 2121–2124.
10. Hu, H.; Elstner, M.; Hermans, J. Proteins Struct Func Genet 2003, 50, 451–463.
11. Field, M. J.; Bash, P. A.; Karplus, M. J Comp Chem 1990, 11, 700–733.
12. Singh, U. C.; Kollman, P. A. J Comp Chem 1986, 7, 718.
13. Warshel, A.; Levitt, M. J Mol Biol 1976, 103, 227–249.
14. MacKerell, J. A. D.; Bashford, D.; Bellott, M.; Dunbrack, R. L., Jr.; Evanseck, J. D.; Field, M. J.; Fischer, S.; Gao, J.; Guo, H.; Ha, S.; Joseph-McCarthy, D.; Kuchnir, L.; Kuczera, K.; Lau, F. T. K.; Mattos, C.; Michnick, S.; Ngo, T.; Nguyen, D. T.; Prodhom, B.; Reiher, I. W. E.; Roux, B.; Schlenkrich, M.; Smith, J. C.; Stote, R.; Straub, J.; Watanabe, M.; Wiorkiewicz-Kuczera, J.; Yin, D.; Karplus, M. J. Phys Chem B 1998, 102, 3586–3616.
15. Cornell, W. D.; Cieplak, P.; Bayly, C. I.; Gould, I. R.; Merz, K. M.; Ferguson, D. M.; Spellmeyer, D. C.; Fox, T.; Caldwell, J. W.; Kollman, P. A. J Am Chem Soc 1995, 117, 5179–5197.
16. Halgren, T. A. J Comput Chem 1996, 17, 616–641.
17. MacKerell, A. D.; Feig, M.; Brooks, C. L. J Am Chem Soc 2004, 126, 698–699.
18. Cramer, C. J.; Truhlar, D. G. Chem Rev 1999, 1999, 2161–2200.
19. Tomasi, J.; Perisco, M. Chem Rev 1994, 94, 2027–2094.
20. Tapia, O. J Math Chem 1992, 10, 139–181.
21. Bader, R. F. W. Atoms in Molecules: A Quantum Theory; Clarendon Press: Oxford, 1990.
22. Bader, R. F. W. Acc Chem Res 1985, 18, 9–15.
23. Bader, R. F. W.; Larouche, A.; Gatti, C.; Carroll, M. T.; MacDougall, P. J.; Wiberg, K. B. J Chem Phys 1987, 87, 1142–1152.
24. Slee, T.; Larouche, A.; Bader, R. F. W. J Phys Chem 1988, 92, 6219–6227.
25. Bader, R. F. W. Chem Rev 1991, 91, 893–928.
26. Stone, A. J. Chem Phys Lett 1981, 83, 233–239.
27. Stone, A. J.; Alderton, M. Mol Phys 1985, 56, 1047.
28. Lorentz, H. A. Theory of Electrons; Dover: New York, 1952.
29. Debye, P. Polar Molecules; Dover: New York, 1929.
30. Sack, V. H. Phys Z 1926, 27, 206–208.
31. Sack, V. H. Phys Z 1927, 28, 199–210.
32. Onsager, L. J Am Chem Soc 1936, 58, 1486–1493.
33. Hassan, S. A.; Guarnieri, F.; Mehler, E. L. J Phys Chem B 2000, 104, 6478–6489.
34. Hassan, S. A.; Mehler, E. L. Proteins: Struct Func Genet 2002, 47, 45–61.
35. Hassan, S. A.; Mehler, E. L.; Zhang, D.; Weinstein, H. Proteins 2003, 51, 109–125.
36. Li, X. F.; Hassan, S. A.; Mehler, E. L. Proteins: Struc Func Bioinf 2004 (in press).
37. Greengard, L. Science 1994, 265, 909.
38. Jackson, J. D. Classical Electrodynamics; Wiley: New York, 1975.

39. Mulliken, R. S. J Chem Phys 1955, 23, 1833–1841.
40. Politzer, P.; Harris, R. R. J Am Chem Soc 1970, 92, 6451.
41. Hirshfeld, F. L. Theor Chim Acta 1977, 44, 129–138.
42. Reed, A. E.; Weinstock, R. B.; Weinhold, F. J Chem Phys 1985, 83, 735–746.
43. Guerra, C. F.; Handgraaf, J. W.; Baerends, E. J.; Bickelhaupt, F. M. J Comp Chem 2003, 25, 189–210.
44. Christoffersen, R. E.; Baker, K. A. Chem Phys Lett 1971, 8, 4.
45. Reed, A. E.; Curtiss, L. A.; Weinhold, F. Chem Rev 1988, 88, 899–926.
46. Stone, A. J.; Alderton, M. Mol Phys 2002, 100, 221–233.
47. Bucher, M.; Porter, T. L. J Phys Chem 1986, 90, 3406–3411.
48. Ehrenson, S. J Comp Chem 1989, 10, 77–93.
49. Mehler, E. L. In Molecular Electrostatic Potential: Concepts and Applications; Murray, J. S.; Sen, K., Eds. Elsevier Science: Amsterdam, 1996, pp 371–405.
50. Böttcher, C. J. F. Physica 1938, 5, 635–639.
51. Hassan, S. A.; Guarnieri, F.; Mehler, E. L. J Phys Chem B 2000, 104, 6490–6498.
52. Mehler, E. L.; Eichele, E. Biochemistry 1984, 23, 3887–3891.
53. Hassan, S. A.; Mehler, E. L. Int J Quantum Chem 2001, 83, 193–202.
54. Hassan, S. A.; Mehler, E. L.; Weinstein, H. In Lecture Notes in Computational Science and Engineering; Hark, K.; Schlick, T., Eds; Springer Verlag: New York, 2002, pp 197–231.
55. Still, W. C.; Tempczyk, A.; Hawley, R. C.; Hendrickson, T. J Am Chem Soc 1990, 112, 6127–6129.
56. Edinger, S. R.; Cortis, C.; Shenkin, P. S.; Friesner, R. A. J Phys Chem B 1997, 101, 1190–1197.
57. Pickersgill, R. W. Protein Eng 1988, 2, 247–248.
58. Mehler, E. L. Protein Eng 1990, 3, 415–417.
59. Haberthur, U.; Majeux, N.; Werner, P.; Caflisch, A. J Comput Chem 2003, 24, 1936–1949.
60. Mehler, E. L. J Phys Chem 1996, 100, 16006–16018.
61. Mallik, B.; Masunov, A.; Lazaridis, T. J Comput Chem 2002, 23, 1090–1099.
62. Scarsi, M.; Apostolakis, J.; Caflisch, A. J Phys Chem B 1997, 101, 8098–8106.
63. Madura, J. D.; Briggs, J. M.; Wade, R. C.; Davis, M. E.; Luty, B. A.; Ilin, A.; Antosiewics, J.; Gilson, M. K.; Bagheri, B.; Scott, L. R.; McCammon, J. A. Comput Phys Commun 1995, 91, 57–95.
64. Ten-no, S.; Hirate, F.; Kato, S. J Chem Phys 1994, 100, 7443–7453.
65. http://cmm.cit.nih.gov/~mago/SCPISM.html.
66. MacKerell, A. D., Jr.; Feig, M.; Brooks, C. L., III. J Am Chem Soc 2004, 126, 698–699.
67. Li, X.; Hassan, S. A.; Mehler, E. L. Biophys J 2004, S86, 412a.
68. Chandler, D. Nature 2002, 417, 491.
69. Huang, D. M.; Chandler, D. J Phys Chem B 2002, 106, 2047.
70. Lum, K.; Chandler, D.; Weeks, J. D. J Phys Chem B 1999, 103, 4570.
71. ten Wolde, P. R.; Chandler, D. Proc Natl Acad Sci USA 2002, 99, 6539–6543.
72. Hassan, S. A. J Phys Chem B 2004, 108, 19501–19509.
73. Lee, C.; Yang, W.; Parr, R. G. Phys Rev B 1988, 31, 785–789.
74. Becke, A. D. J Chem Phys 1993, 98, 5648–5652.